INFLUENCE OF FATIGUE PRE-CRACKING ON ENVIRONMENTALLY ASSISTED FRACTURE OF HIGH-STRENGTH STEEL

V. Kharin and J. Toribio
Department of Materials Engineering, University of Salamanca
E.P.S., Campus Viriato, Avda. Requejo 33, 49022 Zamora
Tel: 980 545 000; Fax: 980 545 002, E-mail: toribio@usal.es

Abstract. This paper analyzes the influence of crack tip plastic strains and compressive residual stresses, created by fatigue pre-cracking, on stress corrosion of steel subjected to localized anodic dissolution or hydrogen assisted fracture. In both situations, cyclic crack tip plasticity improves the behaviour of the material. In the respective cases, the effects are supposed to be due to accelerated local anodic dissolution of the cyclic plastic zone (producing chemical crack blunting) or to the delay of hydrogen entry into the metal caused by residual compressive stresses, thus increasing the fracture load in aggressive environment.

Resumen. Este artículo analiza, en la proximidades del extremo de una fisura, la influencia de las deformaciones plásticas y de las tensiones residuales compresivas, creadas mediante pre-fisuración por fatiga, en la corrosión bajo tensión de aceros sometidos a disolución anódica localizada o fisuración asistida por hidrógeno. En ambas situaciones, la plasticidad cíclica de extremo de fisura mejora el comportamiento del material. En los casos respectivos, los efectos se suponen debidos a la disolución anódica acelerada de la zona plástica cíclica (produciendo redondeo de origen químico del extremo de la fisura) o a la deceleración de la entrada de hidrógeno en el metal como consecuencia de las tensiones residuales compresivas, incrementando de este modo la carga de fractura en ambiente agresivo.

1. INTRODUCTION

Environmentally assisted cracking (EAC) of metals is usually evaluated by testing of pre-cracked specimens prepared by fatigue (cyclic) loading in laboratory air which produces a redistribution of stresses and strains as a consequence of cyclic plastic deformations. Compressive residual stresses generated at fatigue load release, together with plastic strains, affect the stress corrosion behaviour of materials [1].

This paper deals with the mechanical effects of pre-loading on the posterior EAC in a structural steel. The rising load EAC experiments are considered in combination with numerical modelling of the elastoplastic stress-strain field near the crack tip subjected to fatigue pre-cracking and subsequent monotonic loading in EAC tests.

2. EXPERIMENTAL

Experiments were performed with a series of K_{max}/K_{IC}= 0.28, 0.45, 0.60 and 0.80, where K_{IC} is the fracture toughness and K_{max} is the maximum stress intensity factor during fatigue precracking. The EAC experiments were rising load tests of pre-cracked specimens in aqueous solution under anodic and cathodic potentials to evaluate the two main mechanisms of EAC [2]: localized anodic dissolution (LAD) and hydrogen assisted cracking (HAC). The experimental details are described elsewhere [1].

The tested high-strength steel is characterised in Table 1, where fragments of the stress-strain curve σ-ε depend on the plastic strain ε^p. Table 2 presents failure loads in solution F_{EAC} in relation to that in air F_C. For both LAD and HAC, heavier pre-cracking is beneficial for the EAC resistance of the steel. This may be attributed to the cyclic plastic zones and compressive stresses near the crack tip due to fatigue. The higher the cyclic load level, the stronger the pre-straining/stressing effect which delays environmental damage (metal dissolution in LAD or hydrogen entry in HAC) and improves material performance in a hostile environment.

Fractographic analysis of the samples after HAC tests revealed the so called tearing topography surface (TTS) between the fatigue pre-crack and final cleavage rupture. It is a signal of hydrogen assisted microdamage [3].

Measured TTS depth x_{TTS} also depends on the pre-cracking regime (see Table 2).

Table 1. Mechanical properties of the steel.

Young modulus E (GPa)	Tensile yield stress σ_Y (MPa)	Toughness K_{IC} (MPam$^{1/2}$)	Ramberg-Osgood $\varepsilon=\sigma/E+(\sigma/P)^n$ (I) $\varepsilon^p \le 1.07$ P_I (MPa)	n_I	(II) $\varepsilon^p > 1.07$ P_{II} (MPa)	n_{II}
195	725	53	2120	5.8	2160	17

Table 2. Environmentally assisted cracking (EAC) test results as a function of the fatigue pre-cracking regime.

F_{EAC}/F_C (x_{TTS}, μm)	K_{max}/K_{IC} 0.28	0.45	0.60	0.80
LAD	0.70	0.75	0.85	0.99
HAC	0.56 (200)	0.60 (150)	0.66 (85)	0.80 (10)

LAD: anodic regime at – 400 mV vs. SCE
HAC: cathodic regime at – 1200 mV vs. SCE.

3. MODELLING OF CRACK TIP MECHANICS

To ascertain the effects of pre-cracking on EAC, the evolutions of mechanical variables associated with EAC are desired. In previous analyses [4] the superposition approach by Rice [5] was applied to elucidate the elastoplastic stress fields associated with a fatigue crack at maximum and minimum load.

In this paper, a high-resolution numerical modelling of the crack tip stresses and strains during fatigue pre-cracking and rising load EAC test was performed for an elastoplastic material with von Mises yield surface and Ramberg-Osgood strain-hardening rule. Mixed isotropic-kinematic hardening was used to capture Bauschinger-type effects supposedly essential for the modelling of cyclic stress-strain behaviour. Model parameters corresponded to the steel used in the experiments (Table 1).

Finite deformation analysis of a plane strain crack under mode I (opening) load was confined to small scale yielding, so that the stress intensity factor K is the only variable governing the near tip mechanics [6]. The initial crack was modelled as a parallel-sided round-tip slit with initial height b_0 = 5 μm in agreement with data for fatigue cracks in steels [7]. The simulated loading histories consisted of several zero-to-tension cycles with K_{max}/K_{IC}= 0.45, 0.60 and 0.80, followed by rising load representing the EAC tests. An updated Lagrangian formulation was used.

Plastic zones developed fairly self-similar with a scaling factor of $(K/\sigma_Y)^2$, which is natural for the K-dominated crack-tip domain and coincides with the prediction by Rice [5]. At loading up to the first load reversal at K_{max}, the *monotonic plastic zone* is defined by the equivalent von Mises stress $\sigma_{eq} \ge \sigma_Y$ (Fig. 1, left) where σ_Y is the tensile yield stress. The depth of this zone ahead of the crack tip is:

$$x_Y(K_{max}) = 0.0335 \left(\frac{K_{max}}{\sigma_Y}\right)^2 \qquad (1)$$

Because of strain hardening, after load reversal the σ_Y-stress based yield criterion must not indicate further where plastic flow really proceeds. The *cyclic plastic zones* are defined then by positive equivalent plastic strain rate, $\xi_{eq}^p > 0$ (Fig. 1, right). They are approximately the same at cyclic load minima (*reversed* zones at K_{min} = 0) and maxima (*forward* zones at K_{max}), smaller than the monotonic zone and quite stable with the cycle number. The depth of this zone of cyclic accumulation of plastic strain is:

$$\Delta x_Y(K_{max}) = 0.0065 \left(\frac{K_{max}}{\sigma_Y}\right)^2 \qquad (2)$$

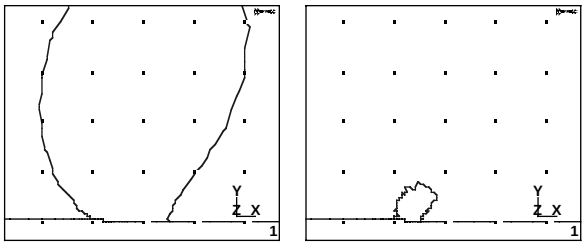

Fig. 1. Monotonic plastic zone (left) and cyclic plastic zone (right) at $K = K_{max}$ for the loading history with K_{max}/K_{IC} = 0.6 (the grid spacing is 50 μm).

At rising load next to cyclic load release, plastic flow starts at $K \approx 0.2K_{max}$ after elastic reloading and develops identically as the cyclic zone does up to attaining the pre-cracking level of $K = K_{max}$, when it bursts and advances as the monotonic one. Thus the active plastic zone (APZ) depth during EAC test is:

$$x_{APZ}(K) = \begin{cases} 0 & \text{at } K \lesssim 0.2K_{max} \\ \Delta x_Y(K) = 0.19 x_Y(K) & \text{at } 0.2K_{max} \lesssim K \le K_{max} \\ x_Y(K) & \text{at } K > K_{max} \end{cases} \qquad (3)$$

The near tip stress distributions differ substantially from estimation given by Rice [5] They stabilise after few first cycles as soon as a steady state of alternating plastic flow is approached. Fig. 2 shows the evolution of the hydrostatic stress in the crack plane beyond the tip, $\sigma = \sigma(x)$, where x is the distance to the crack tip in the deformed configuration of a solid, during monotonic loading in the EAC test after pre-cracking. This stress component is focused since it is determinant for HAC controlled by stress-assisted hydrogen

diffusion driven by the gradient $\nabla\sigma$ towards maximum tension locations [8,9]. With regard to the normal stress in the plane of the crack σ_{yy} potentially responsible for tensile rupture, the patterns of $\sigma_{yy}(x)$ were quite similar to those in Fig. 2. For both stresses, their extrema (local minima and maxima) are placed roughly at the same depths $x_{\sigma-}$ and $x_{\sigma+}$, respectively, and $\sigma_{yy} \approx 1.6\sigma$ at $x \lesssim$ (2 to 3) $x_{\sigma+}$, these distances being shorter than those predicted by Rice [5].

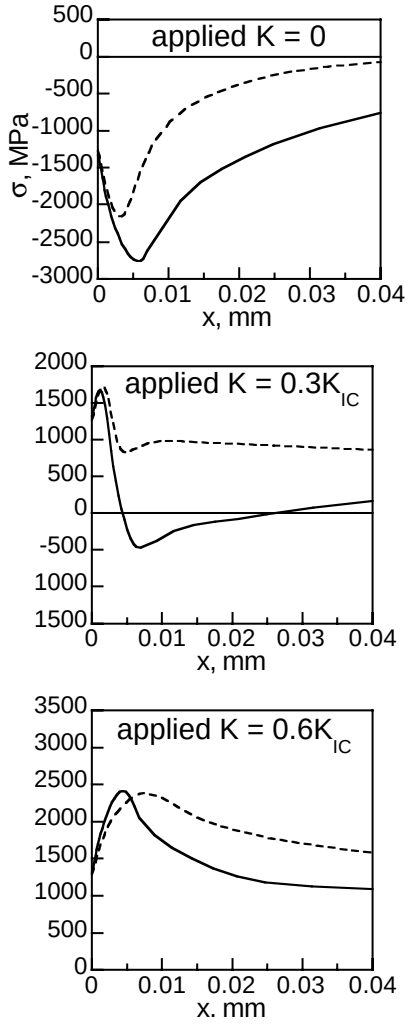

Fig. 2. Hydrostatic stress distributions beyond the crack tip during monotonic loading at EAC test after fatigue pre-cracking at K_{max}/K_{IC} = 0.45 (dashed lines) and 0.80 (solid lines),

4. DISCUSSION

To analyze the results of the EAC tests on the basis of crack tip mechanics, the critical stress intensity factor for EAC to proceed K_{QEAC} is evaluated from the experimental failure loads (Table 2) as follows:

$$K_{QEAC} = \frac{F_{EAC}}{F_C} K_{IC}(air) \qquad (4)$$

For LAD-controlled fracture, fatigue pre-cracking may cause a strong protective effect characterised by the fracture loads ratio F_{EAC}/F_C (Table 1). Considering mechanical factors of EAC, the normal stresses at the crack tip surface (at x = 0) and the crack tip plastic strains may influence LAD processes [2]. Evolutions of the crack tip mean normal stress $\sigma(x = 0)$ during EAC after different pre-cracking regimes (Fig. 3a) are practically insensitive to the cyclic load level K_{max}. Stresses in the interior at x > 0 must be irrelevant for LAD since it is a surface dissolution reaction. Therefore, no difference should be expected for LAD from the residual stresses produced at different K_{max}.

Toughening effect of the pre-cracking on LAD-driven EAC may be associated with accelerated dissolution of the cyclic plastic zone due to the inherently higher chemical activity of its damaged crystalline structure [2]. Due to cyclic damage accumulation not only ahead of the tip but also aside of the main crack path (Fig. 1), lateral strain-enhanced dissolution may allow chemical crack blunting to compete with dissolution-induced crack extension. Then, fracture load must increase together with the LAD-driven crack blunting. The LAD process may be supposed to involve a domain with a cumulative plastic strain above a certain level. This region must be proportional to the zone of accumulated cyclic plastic strain Δx_Y, or probably to the active plastic size x_{APZ} which during a notable portion of the EAC test route coincides with the former, cf. eq. (3). Fig. 3b displays this correspondence according to the EAC tests and numerical data about plastic zones.

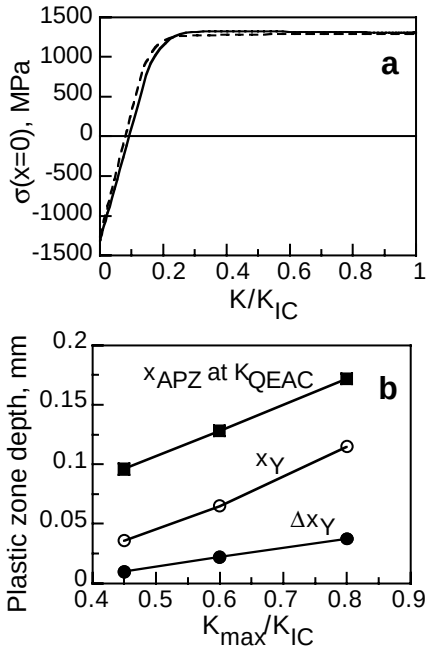

Fig. 3. Mechanical factors of the crack growth by LAD: (a) evolutions of the crack tip hydrostatic stress σ during EAC test after fatigue pre-cracking at K_{max}/K_{IC} = 0.45 (dashed line) and 0.80 (solid line); (b) sizes of the plastic zones associated with EAC tests: the terminal active plastic zone during the LAD test (x_{APZ} at K_{QEAC}) which surpasses the cyclic and the monotonic plastic zones created during fatigue pre-cracking of the specimens, $\Delta x_Y(K_{max})$ and $x_Y(K_{max})$ respectively.

For HAC-controlled fracture, hydrogen transport to prospective rupture sites ahead of the crack tip may be supplied by two different mechanisms [8,9]. (i) sweeping by moving dislocations within the active plastic zone during load rise; (ii) diffusion in metal driven by hydrostatic stress gradient $\nabla\sigma$ towards the maximum tensile stress locations.

With regard to the first, hydrogenation and hydrogen damage area must be about as extensive as the active plastic zone. However, experimental data on the TTS width x_{TTS} as an indicator of hydrogen damage (Table 2) do not agree with calculated plasticity extent x_{APZ} after different pre-cracking regimes (Fig. 4a). Although TTS overpassing the plastic zone size at lower K_{max} levels in Fig. 4a may be attributed to the subcritical crack growth and plastic (damage) zone displacement next to the crack tip, it cannot be at $K_{max} = 0.8K_{IC}$ when $x_{TTS} << x_{APZ}$ even for stationary crack. This fact indicates that dislocational transport of hydrogen must not be the responsible for HAC in this case.

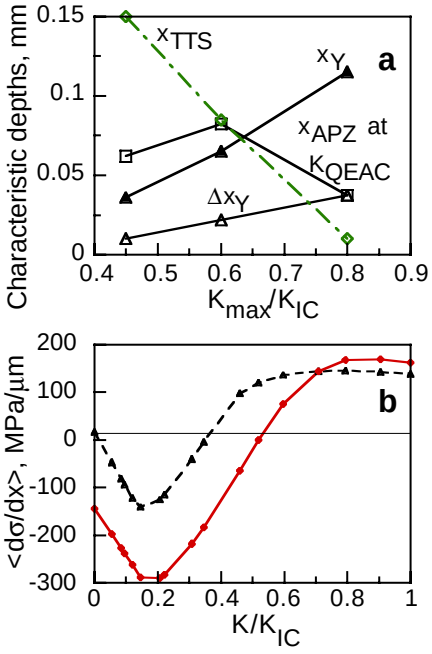

Fig. 4. Mechanical factors of the crack growth by HAC: (a) comparison of the TTS extension and the plastic zones associated with HAC tests: at lower K_{max}-levels, the terminal active plastic zone (open square points) at the end of the HAC test (x_{APZ} at K_{QEAC}) surpasses the cyclic and the monotonic plastic zones created during fatigue precracking (triangles), $\Delta x_Y(K_{max})$ and $x_Y(K_{max})$ respectively; (b) evolutions of the average value of the hydrostatic stress gradient during HAC tests after fatigue pre-cracking at $K_{max}/K_{IC} = 0.45$ (dashed line) and 0.80 (solid line).

Considering stress-assisted diffusion, the near tip distributions of the hydrostatic stress $\sigma(x)$ in Fig. 2 indicate that, during the rising load EAC tests, initially compressive stresses $\sigma(x) < 0$ and accompanying negative gradients $d\sigma/dx < 0$ induced by fatigue pre-cracking delay hydrogen penetration towards rupture sites, and this effect is more pronounced for the heaviest fatigue regimes (i.e., with the highest K_{max}). This is supported by comparison of the evolutions of the average value of the stress gradient $\langle\nabla\sigma\rangle$ over the range $0 \le x \le x_{\sigma+}(K_{QEAC})$ (Fig. 4b) which delays hydrogen transportation into the metal as far as the respective component of the diffusion flux is $\mathbf{J}_\sigma \propto \nabla\sigma$ [8,9]. This scale of averaging $x_{\sigma+}(K_{QEAC})$ corresponds to the maximum tensile stress position and possible location of the stress-controlled microfracture at hydrogen induced failure in experiments. For the precracking regimes compared in Fig. 4, this distance is fairly the same $x_{\sigma+}(K_{QEAC}) = 8$ μm, so that it may be supposed to be a characteristic microstructural scale for HAC. Therefore, the heaviest fatigue pre-cracking regimes delay the hydrogen accumulation, and correspondingly the progress of hydrogen degradation in the course of a rising load EAC test.

5. CONCLUSIONS

Environmentally-assisted fracture of high-strength steel is clearly influenced by fatigue pre-cracking, since cyclic loading affects plastic strains and creates compressive residual stresses in the vicinity of the crack tip.

Cyclic accumulation of plastic strain and compressive residual stresses improve the EAC behaviour through increase of the failure load in aggressive environment either by chemical blunting of the crack tip enhanced by accumulated plastic strain (in LAD) or by delaying hydrogen supply to the fracture process zone near the crack tip by stress-assisted diffusion (in HAC).

Acknowledgments

The financial support (Grant MAT2002-01831) of this work by the Spanish Ministry of Science and Technology (MCYT) and FEDER is gratefully acknowledged. In addition, the authors wish to express their gratitude to EMESA TREFILERIA S.A. for providing the steel used in the experimental programme.

REFERENCES

[1] Toribio, J. and Lancha, A.M., "Overload retardation effects on stress corrosion behaviour of prestressing steel", *Construction and Building Materials* **10**, 501-505 (1996).

[2] Ford, F.P., "Stress corrosion cracking of iron-base alloys in aqueous environments", in: *Treatise on Materials Science and Technology*, *Vol. 25: Embrittlement of Engineering Alloys* (Edited by C.L. Briant and S.K. Banerji), Academic Press, New York, 235-274 (1983).

[3] Toribio, J., Lancha, A.M. and Elices, M., "Characteristics of the new tearing topography surface", *Scripta Metallurgica et Materialia* **25**, 2239-2244 (1991).

[4] Toribio, J. and Lancha, A.M., "Effect of cold drawing on susceptibility to hydrogen embrittlement of prestressing steel", *Materials and Structures* **26**, 30-37 (1993).

[5] Rice, J.R., "Mechanics of crack tip deformation and extension by fatigue.", in: *Fatigue Crack Propagation*, *ASTM STP 415*, American Society for Testing and Materials, Philadelphia 247-309 (1967).

[6] Kanninen, M.F. and Popelar, C.H., *Advanced Fracture Mechanics*, Oxford University Press, New York (1985).

[7] Handerhan, K.J. and Garrison, W.M., Jr., "A study of crack tip blunting and the influence of blunting behavior on the fracture toughness of ultra high strength steels", *Acta Metallurgica et Materialia* **40**, 1337-1355 (1992).

[8] Van Leeuwen, H.-P., "The kinetics of hydrogen embrittlement: a quantitative diffusion model", *Engineering Fracture Mechanics* **6,** 141-161 1974).

[9] Toribio, J. and Kharin, V., "*K*-dominance condition in hydrogen assisted cracking: the role of the far field", *Fatigue and Fracture of Engineering Materials and Structures* **20**, 729-745 (1997).